






Dielectric and Conductivity Study of Salt-Doped HPMC Solid Polymer Electrolyte Films

Sunil Kumar^{1,2} , Sandhya Rani Nagarajaiah³ , Raghu S⁴ , Sandeep Dongre¹ ,
Demappa Thippaiah⁵ , Sannappa Jادیappa^{1,*} 

¹ Department of P G Studies and Research in Physics, Jnana Sahyadri, Kuvempu University, Shivamogga 577451, India; sannappaj2012@gmail.com (S.J.);

² Department of Physics, S.S Arts College and T.P Science Institute, Sankeshwar, Belagavi 591313, India; sunil11111kumar@gmail.com (S.K.);

³ Department of Physics, Vidyavardhaka College of Engineering, Mysore 57002, India; sandhya.phy@vvc.ac.in (R.N.S.);

⁴ Department of Physics, KLE Society's, Basavaprabhu Kore Arts, Science and Commerce College, Chikodi 591201, India; raghu.mona@gmail.com (R.S.);

⁵ Department of Polymer Science, Sir M V, P G Centre, University of Mysore, Mandya 571402, India; demappa@uni-mysore.ac.in (D.T.);

* Correspondence: sannappaj2012@gmail.com (S.J.);

Scopus Author ID 6508209624

Received: 27.08.2022; Accepted: 7.10.2022; Published: 5.02.2023

Abstract: This study reports the solid polymer electrolyte films of hydroxypropyl methylcellulose (HPMC) doped with different sodium bromide (NaBr) salt concentrations. The test samples were prepared using the solution cast method, and their structural characterization was done using XRD, SEM, and FTIR. Sharp crystalline peaks of pure NaBr salt disappeared completely in all the HPMC:NaBr polymer electrolyte systems revealing the reduced crystallinity, which greatly influences the dielectric and conductivity of the polymer electrolytes. Fourier transform infrared spectral (FTIR) reports subjected to vibrational changes that appeared due to the result of dopant salt in the host polymer. The samples were analyzed using a pc-based impedance analyzer (Wayne Kerr 6510B) in the frequency scale of 50 Hz to 1 MHz. As the frequency increases, the constant dielectric declines, and the AC electrical conductivity rises. The AC conductivity curves in the high-frequency area follow the Jonscher Power Law. The electrolyte's non-Debye behavior was supported by its relaxation time and dielectric property. According to the reported polymer electrolyte systems, the distribution of relaxation time is influenced by the presence of conducting ions in an amorphous formation. All assessed outcomes of these polymer electrolytes are assuring their use for electrochemical cell drives.

Keywords: solid polymer electrolyte; dielectric constant; ac conductivity; impedance analysis.

© 2022 by the authors. This article is an open-access article distributed under the terms and conditions of the Creative Commons Attribution (CC BY) license (<https://creativecommons.org/licenses/by/4.0/>).

1. Introduction

Supercapacitors (SCs), fuel cells, batteries, and other energy conversion and storage technologies primarily employ solid polymer electrolytes (SPEs) [1-4]. SPEs are composed of dissolved salts in high molecular mass polymer matrices. Compared to other liquid ionic solutions, the ionic-conducting phase of SPEs has a better transport property. Additionally, they are flexible, light in weight, relatively high in ionic conductivity, solvent-free, and capable of forming films. Likewise, they are risk-free and also leakage free. In 1973, poly(ethylene oxide) (PEO) that had been combined with alkali metal salts was the first ion-conducting polymer to be reported [5]. J Koliyoor *et al.* studied Magnesium ion-doped methyl cellulose

electrolyte system and found the highest ionic conductivity of 1.02×10^{-4} S/cm at room temperature for 25 wt% Mg [6]. Bashir A.A. *et al.* reported the highest conductivity of 5.30×10^{-4} S/cm for Poly (vinyl alcohol) (PVA) and cellulose acetate (CA) in 80:20 with 20 wt% potassium carbonate [7]. N. M. Khan *et al.* reported AL-NH₄Cl BE's highest ionic conductivity of 3.18×10^{-8} S/cm for an NH₄Cl content of 8 wt%. However, when plasticized with 4 wt% of EC, an increased optimum value of 1.46×10^{-6} S/cm was obtained [8]. Maheshwari *et al.* reported a maximum conductivity of 1.66×10^{-3} S/cm at room temperature for the composition 700 mg_{Dextran}:300 mg_{PVA}:450 mg_{NH₄NO₃} [9]. The ion transport property depends on various factors, including a degree of ion aggregation, salt concentration, degree of salt dissociation, polymer chain mobility, etc. Even though the SPEs have good conductivity, the analysis of dielectric studies gives additional information for understanding ion transport actions and getting data on molecular/ionic interface in polymer electrolytes [10]

In contrast to other cellulose derivatives (carboxymethylcellulose, hydroxyethyl cellulose (HEC), and methylcellulose (MC)), HPMC is more thermally stable, making it the preferred host polymer. It is widely utilized in the textile, biomedical, and pharmaceutical industries because it is biodegradable and non-toxic [11-13]. According to earlier research, HPMC can dissolve various metal salts and produce thin films with exceptional stability [12,13]. Compared to other inorganic salts, the benefit of using sodium metal particles is their abundance and accessibility at a low cost [14-18]. The inorganic compound sodium bromide (NaBr) is a white crystalline solid with a high melting point. It is a widely used source of bromide ions in pharmaceutical preparations [19]. As a result, the sodium-ion battery has gained popularity as the next-generation secondary battery because it is much less expensive than a lithium-ion battery. Several research findings have found that Na⁺ ions bring better or comparable ionic conductivity to Li⁺ ions in the same primary host source [20-21]. This presented a chance to develop a battery using Na⁺ ions instead of lithium. NaBr does have narrow lattice energy of 747 kJ/mol, that's a little less than NaCl (786 kJ/mol) because Br (182 pm) is larger than Cl (167 pm) [22]. The lattice energy of salts and the crystalline percentage of sodium salts used in PEs can significantly impact the synthesized electrolyte's conductivity. As a result, this study looks into the effect of NaBr salt on the dielectric and electrical conductivity properties of HPMC-based solid polymer electrolytes.

2. Materials and Methods

The electrolyte film samples are prepared by the standard casting method. The samples in pure form are purchased from Sigma-Aldrich. Here water is used as a base solvent, and different percentages of samples are prepared. Initially, the pure film is prepared by adding 3 grams of HPMC in 100 ml double distilled water, and it is let to stir for 24 hours. The prepared solution is poured into the glass slab (14x14 cm), and it is dried for 7-10 days. Finally, the film samples are peeled from the glass slab and kept in the desiccators to avoid moisture.

Similarly, different percentages of salt are added to the pure solution. Experiments like XRD, FTIR, and SEM assessed the synthesized pure HPMC and doped HPMC polymer electrolyte films. These samples' dielectric and AC conductivity were measured using a PC-based impedance analyzer at frequencies from 50 Hz to 1 MHz (Wayne Kerr 6510B).

3. Results and Discussion

3.1. Structural study.

Our previous paper described the structural evaluation of the prepared polymer electrolyte films. According to Figure 1, the Virgin HPMC film showed a pronounced peak that occurred at 22.17° , revealing the semi-crystalline character of HPMC, and this broad peak disappeared in the NaBr salted HPMC films. The crystallinity decreased with salt content in doped films, indicating a decrease in intermolecular interaction (crystalline phase) [23].

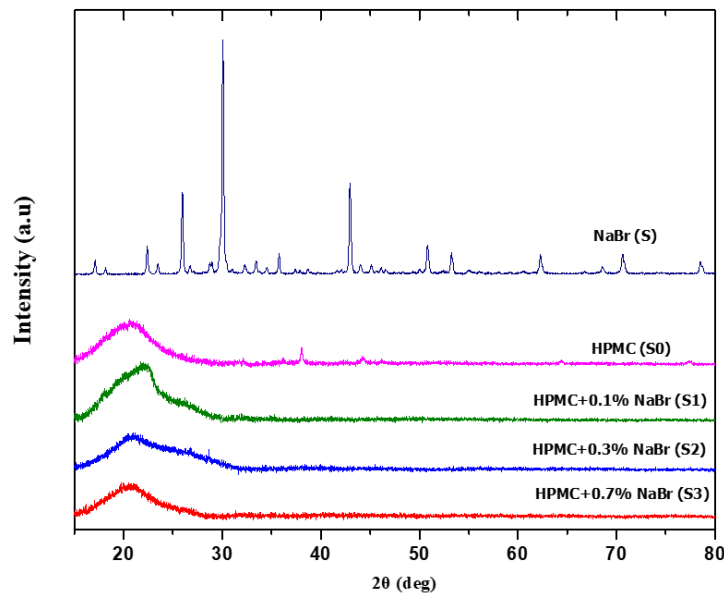


Figure 1. XRD Spectrum of pure and NaBr doped samples [23].

3.2. FTIR studies.

In our earlier paper, we reported on the evaluation of the IR spectra of the prepared composite film samples.

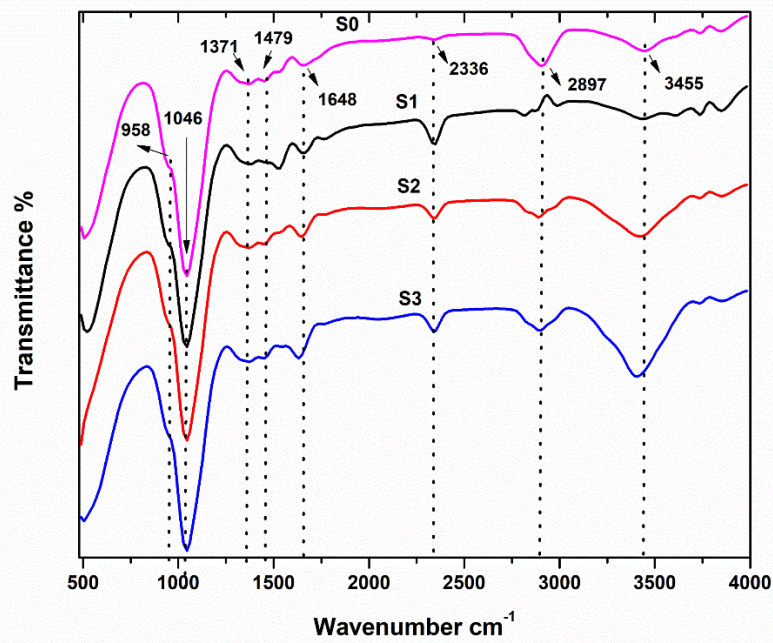


Figure 2. FTIR Spectrum of pure and NaBr doped samples [23].

The effect of the dopant on the vibration modes was observed in the IR spectra as a decrease in intensities, a widening of the bands, and repositioning of the bands to shorter wavenumbers. All of these variations in the FTIR spectra are dependable signs of polymers-ion complexes. The OH groups are vital for ensuring the crystalline packing of the polymer [24]. The large shift and variation in the OH group's intensity in complex films causes a break of the crystalline phase and simultaneously increases amorphous content [23].

3.3. SEM studies.

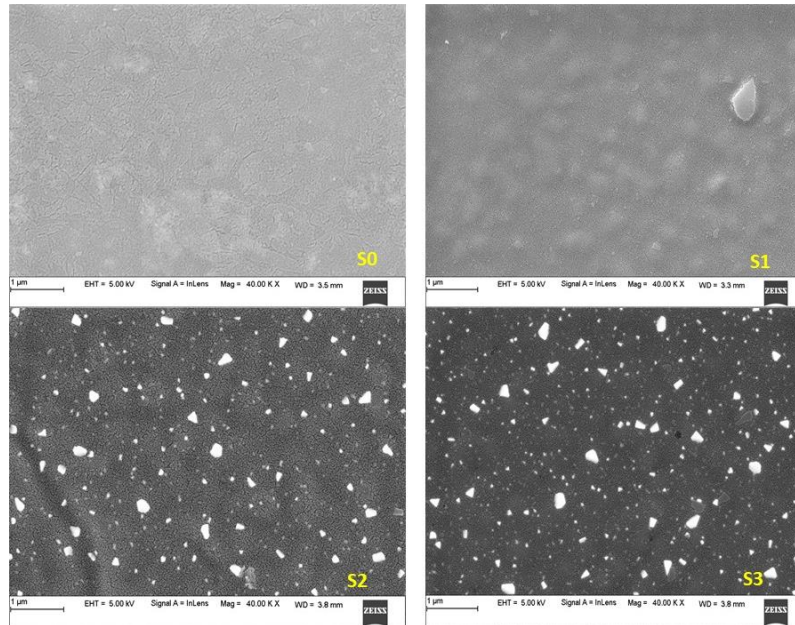


Figure 3. SEM Spectrum of pure and NaBr doped samples [20].

The SEM results of the ready composite film sample were reported in our earlier paper. Pure HPMC film can show plane morphology [12]. The complex film samples display varying degrees of roughness, which shows the dopant has segmented in the host polymer matrix and broken up its crystalline phase [23].

3.4. Conductivity and dielectric studies.

3.4.1. Room temperature study of complex impedance spectroscopy analysis.

The following equation 1 [25] gives the complex impedance (Z^*) based on impedance modulus (Z' and Z'').

$$Z^* = Z' + iZ'' \tag{1}$$

where Z' represents the real part of the impedance modulus and Z'' represents the imaginary part, as given by equations 2 and 3

$$Z' = \frac{1}{2\pi f C_o} \left[\frac{\epsilon''}{\epsilon''^2 + \epsilon'^2} \right] \tag{2}$$

$$Z'' = \frac{1}{2\pi f C_o} \left[\frac{\epsilon'}{\epsilon''^2 + \epsilon'^2} \right] \tag{3}$$

where C_0 is the vacuum capacitance, and f is the frequency. The ϵ' and ϵ'' are real and imaginary parts of dielectric permittivity, respectively.

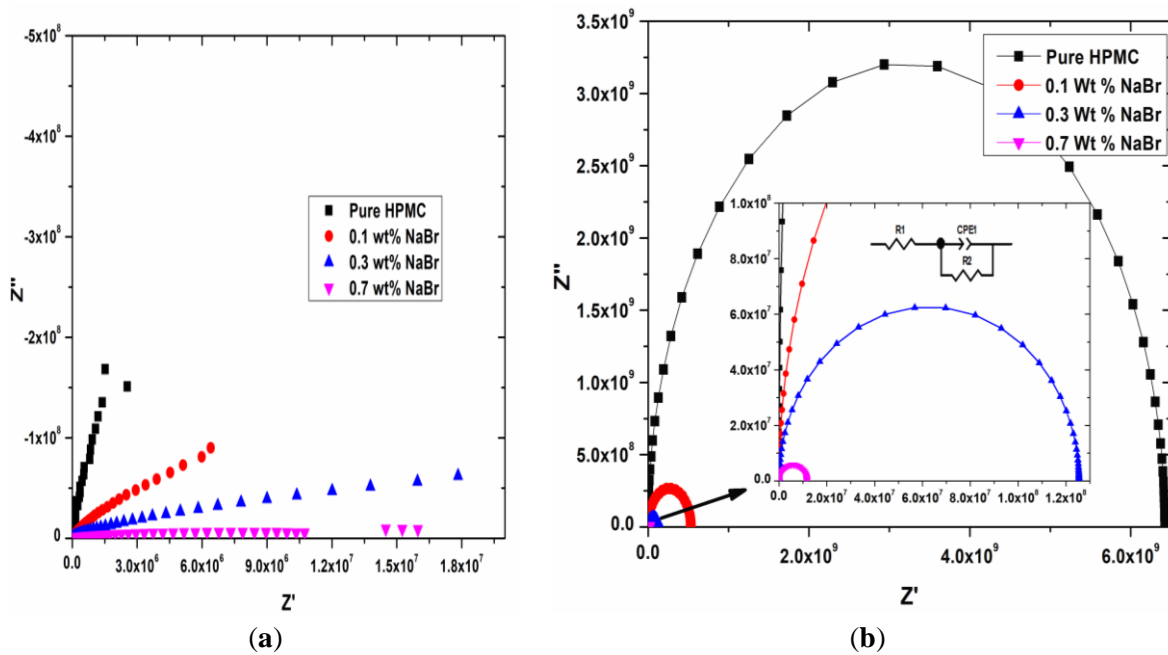


Figure 4. (a) Plot of Complex impedance Nyquist. (b) electrical equivalent circuit for pure and doped electrolyte samples at room temperature.

Figure 4 (a) shows the complex impedance plots of Z^* (known as Nyquist plot) at room temperature for pure and doped samples. The complex impedance Figure 4a shows an inclined spike which shows the interaction of two blocking electrodes, which triggers the formation of double-layer capacitance of HPMC:NaBr film [26-28]. Figure 4 (b) displays the experimental data fitted plots that were developed using an equivalent circuit consisting of a resistance R_1 (grain resistance R_g) in series with a fixed phase impedance (Z_{CPE}) and resistance R_2 (grain boundary resistance R_{gb}) in parallel. The analogous composition is of the form $\left(R_1 + \left(R_2 / Z_{CPE} \right) \right)$. Table 1 displays the values of all fitted parameters. From the plots, it is clear that the R_b value declines with increasing NaBr salt. All samples display a high-frequency semi-circle arc that is connected to the bulk conduction process [26,27].

The assessment of Argand sketches with a complete semi-circular arc on the real impedance (Z') axis discloses that relaxation time varies for charge carriers [28]. From Table 1, the R_g value declines with the rise of NaBr concentration and achieves the lowest value ($1.607 \times 10^7 \Omega$) for HPMC/NaBr 0.7 wt % sample. Hence, 0.7 wt % NaBr content composite polymer electrolyte has a significant ionic conductivity. The density and mobility of charge carriers both contribute to the variation in the ionic conductivity of electrolyte samples [29].

3.4.2. Dielectric analysis.

A detailed study of the dielectric constant is required to design and advance electrical and electronic components. It exposes more knowledge about the polymer's physical and chemical state. When contrasted to ceramic materials, it is possible to create polymers with good dielectric constants and small dielectric losses [30]. Figure 5 depicts the room temperature dielectric constant (real part ϵ') and $\text{Log}(f)$ plots for pure and doped electrolyte systems for frequencies stretching from 100 Hz to 1 MHz.

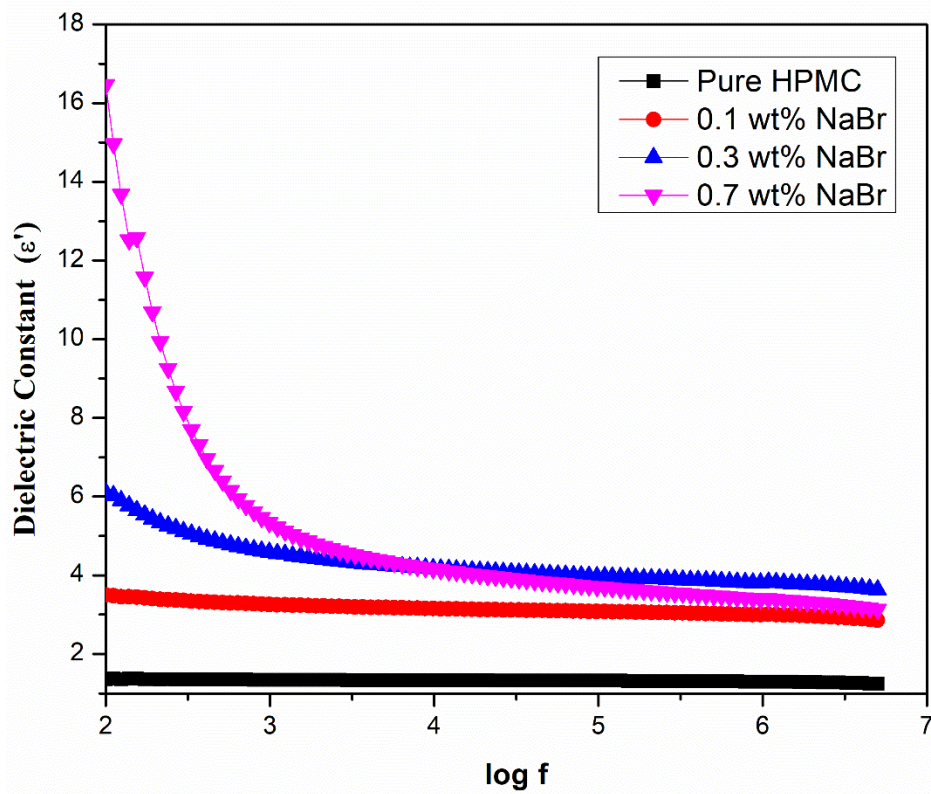


Figure 5. Variation of Dielectric constant (ϵ') with frequency.

The relationship used to calculate the dielectric constant is given by equation 4

$$\epsilon' = \frac{Cd}{\epsilon_0 A} \tag{4}$$

where 'C' stands for equivalent capacitance, 'd' for sample thickness, ϵ_0 for free-space permittivity, and "A" for sample area.

Figure 5 plots clearly show that the dielectric constant falls as frequency rises. NaBr salt has a noticeable impact on the dielectric constant at room temperature, resulting in an increase in total charge carriers, dielectric constant, and ionic conductivity. The outcome displays that the host polymer electrolyte complexed with 0.7 wt % NaBr salt reports a high dielectric constant and shows the maximum ionic conductivity. The increase in the dielectric constant at short frequencies is caused by the space charge polarization at the electrode-electrolyte junction. This charge growth displays relaxation behavior resembling dipolar relaxation [31]. Due to the presence of space charge polarisation at the electrode-electrolyte junction, there is a high dielectric constant at low frequencies. This shows that the applied electric field periodically reverses that no longer be followed by the dipoles [32,33]. As a result, as the frequency rises, the charge carriers' contribution to polarisation also declines, which results in a continuous decline in the ϵ' - values.

3.4.3. AC electrical conductivity.

The scaling of dielectric properties with frequency under conditions of alternating current (AC) is given by Power law equation 5.

$$\sigma(\omega) = \sigma_{dc} + A\omega^S \tag{5}$$

Here, $A\omega^s$ is the only dispersive AC conductivity factor that appears in the power law form of angular frequency (ω), and s is the power element ($0 \leq s \leq 1$), denotes how well mobile ions interface with the lattices surrounding those. A is a constant that determines the strength of polarizability. Exponent factor s $\sigma(\omega)$ is the total conductivity, and σ_{dc} is the DC conductivity of the sample. Table 1 shows the room temperature assessment of parameters attained from JPL fit (Equation 7) with the experiment records of electrolyte samples. Figure 6 displays that the AC conductivity at room temperature rises with frequency and reaches a maximum for the highest doped electrolyte of 0.7 wt % HPMC-NaBr. The frequency-dependent electrical conductivity of polymer-electrolyte obeys Jonscher Power Law (JPL) [34-36]. The JPL fitting and the experimental values match each other well. The plateau region in the low frequency relates to σ_{dc} . The conductivity in the large-frequency province obeys $A\omega^s$. Jonscher claims that the cause of the frequency dependency of conductivity is the cause of mobile charge carriers payable to the relaxation existences of the ionic atmosphere. In the host polymer matrix, ions jump from one vacant site to an adjacent vacant site, contributing to DC conductivity at lower frequencies. This effective ion hopping occurs at a shorter frequency than the hopping frequency. The figure shows higher frequencies exhibit more dispersive conductivity due to the ions' backward and forward hopping motion [37].

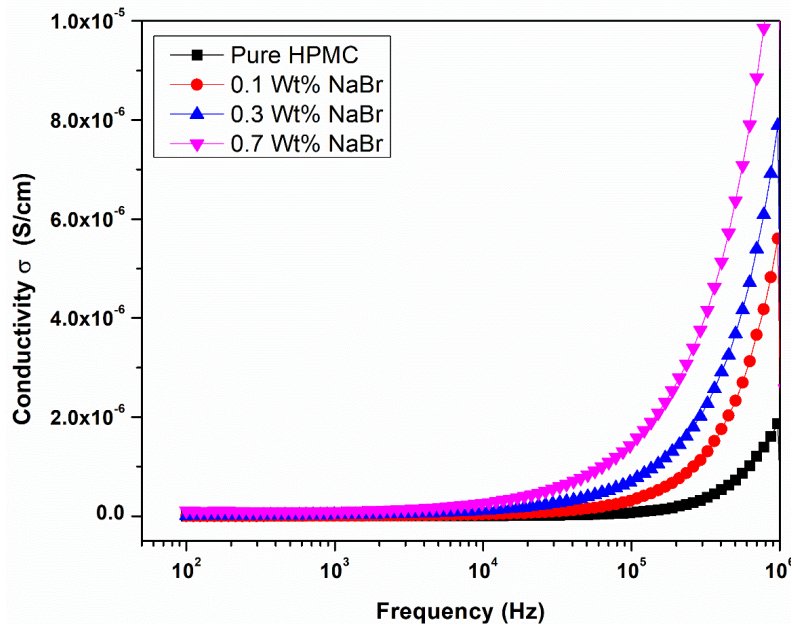


Figure 6. Variation of AC conductivity versus frequency.

Table 1. Variation of Grain resistance, capacitance, relaxation time, ac conductivity, and dc conductivity with salt concentration at room temperature.

Parameters	Pure HPMC	0.1 wt% NaBr	0.3 wt% NaBr	0.7 wt% NaBr
R_g (k Ω)	6.4325×10^9	5.314×10^8	1.255×10^8	1.607×10^7
C (F)	8.348×10^{-12}	1.632×10^{-11}	1.927×10^{-11}	2.645×10^{-11}
τ (s)	1.591×10^{-3}	1.427×10^{-3}	1.279×10^{-3}	3.45×10^{-4}
σ (S/cm)	1.87005×10^{-6}	5.60342×10^{-6}	7.8932×10^{-6}	1.23638×10^{-5}
S	1.01374	0.86887	0.69948	0.51776
σ (dc)	1.5019×10^{-10}	1.629×10^{-9}	1.1154×10^{-8}	1.094×10^{-7}

3.4.4. Complex electrical modulus analysis at room temperature.

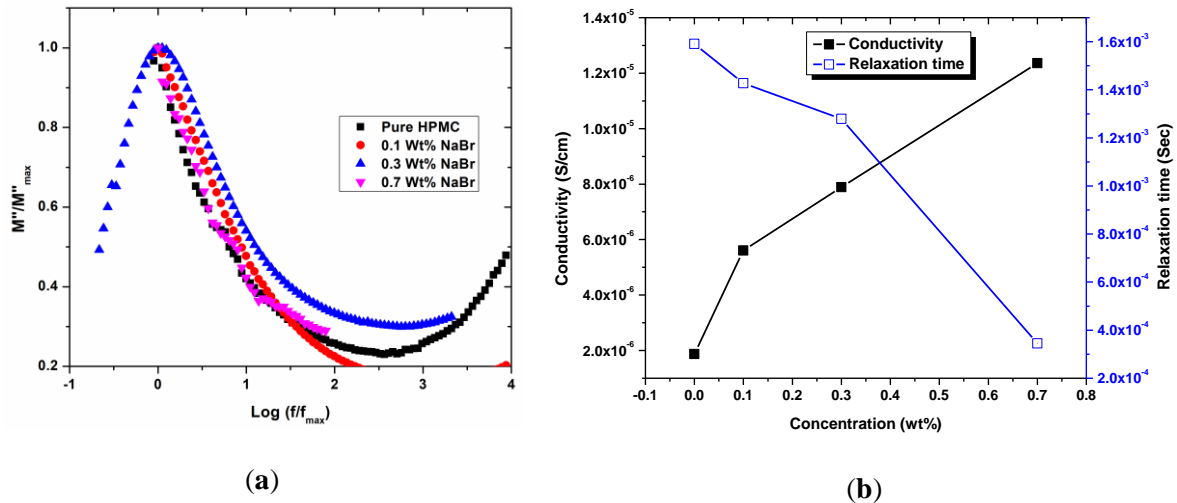


Figure 7. (a) Normalized plot of M''/M''_{max} versus $\text{log}(f/f_{max})$; (b) Variation of relaxation time with dopant concentration.

Theoretically, the complex electrical modulus is derived from the complex permittivity M^* using equation 6 [38].

$$M^* = M' + iM'' \tag{6}$$

The real M' and imaginary M'' parts of the dielectric modulus can be calculated from ϵ' and ϵ'' using equation 7 and 8 as follows:

$$M' = \left[\frac{\epsilon'^2}{\epsilon'^2 + \epsilon''^2} \right] \tag{7}$$

$$M'' = \left[\frac{\epsilon''^2}{\epsilon'^2 + \epsilon''^2} \right] \tag{8}$$

The relaxation time can be calculated from the peak position of M'' using equation 9:

$$\tau = \frac{1}{2\pi f_{max}} \tag{9}$$

where f_{max} is the frequency corresponding to the maximum peak position of the plot.

From Figure 7 (a), all samples' curve peaks overlap, suggesting the relaxation shows the same mechanism. The peak shifts slightly towards a higher frequency as the dopant salt concentration increases, indicating a decrease in relaxation time and resulting in maximum ionic conductivity. The spread of relaxation and non-Debye-type behavior in these electrolyte film samples is confirmed by the asymmetric broadening of the peak [39]. Figure 7 (b) shows the room temperature variation of relaxation time. The relaxation time decreases with the dopant. The lowest relaxation time was observed in the highest wt% film sample.

4. Conclusions

The chemical and physical parameters of polymer electrolytes are dependent on the degree of crystallinity. XRD and FTIR characterizations confirmed the complexation of salt in the host polymer. The structural results showed a significant decrease in crystallinity in the

host polymer with salt concentration because additional salt prevents polymer chains from crystallizing. SEM images of composite films show more degree of roughness compared to the host polymer. The intensity variation and shift in the band were observed through functional studies, which signifies the host polymer's interaction with NaBr. It has been found that increases in AC electrical conductivity depend on frequency. The AC conductivity plots in the high-frequency region show Jonscher's power law. The dielectric property and relaxation time confirmed the non-Debye behavior of the electrolyte system. The distribution of relaxation times is related to the presence of conducting ions in an amorphous structure of the reported polymer electrolyte systems. The estimated outcomes strongly support the use of these polymer electrolytes in electrochemical cell electronic applications.

Funding

This research received no external funding.

Acknowledgments

The author, Sunil Kumar, is thankful to the Physics department, Kuvempu University and S S Arts College, and T P Science Institute for providing sample preparation and characterization facilities.

Conflicts of Interest

The authors declare no conflict of interest. The authors declare that they have no known competing financial interests or personal relationships that could have appeared to influence the work reported in this paper.

References

1. Asnawi, A.; Hamsan, M.; Aziz, S.; Kadir, M.; Matmin, J.; Yusof, Y. Impregnation of [Emim] Br ionic liquid as plasticizer in biopolymer electrolytes for EDLC application. *Electrochim. Acta.* **2021**, *375*, 137923, <https://doi.org/10.1016/j.electacta.2021.137923>.
2. Aziz, S.; Dannoun, E.; Hamsan, M.; Abdulwahid, R.; Mishra, K.; Nofal, M.; Kadir, M. Improving EDLC Device Performance Constructed from Plasticized Magnesium Ion Conducting Chitosan Based Polymer Electrolytes via Metal Complex Dispersion. *Membranes.* **2021**, *11*, 289, <https://doi.org/10.3390/membranes11040289>.
3. Aziz, S.; Nofal, M.; Kadir, M.; Dannoun, E.; Brza, M.; Hadi, J.; Abdullah, R. Bio-Based Plasticized PVA Based Polymer Blend Electrolytes for Energy Storage EDLC Devices: Ion Transport Parameters and Electrochemical Properties. *Materials.* **2021**, *14*, 1994, <https://doi.org/10.3390/ma14081994>.
4. Aziz, S.; Asnawi, A.; Kadir, M.; Alshehri, S.; Ahamad, T.; Yusof, Y.; Hadi, J. Structural, Electrical and Electrochemical Properties of Glycerolized Biopolymers Based on Chitosan (CS): Methylcellulose (MC) for Energy Storage Application. *Polymers* **2021**, *13*, 1183, <https://doi.org/10.3390/polym13081183>.
5. Agrawal, R.C.; Pandey, G.P. Solid polymer electrolytes: Materials designing and all-solid-state battery applications: An overview. *J. Phys. D Appl. Phys.* **2008**, *41*, 223001. <https://doi.org/10.1088/0022-3727/41/22/223001>.
6. Koliyoor, J.; Ismayil; Hegde, S.; Vasachar, R.; Sanjeev, G. Novel solid biopolymer electrolyte based on methyl cellulose with enhanced ion transport properties *J. Appl. Polym. Sci.* **2022**, *139*, 51826, <https://doi.org/10.1002/app.51826>.
7. Bashir, A.A.; John, O.D.; Abbas, A.A.; Yerima, M.H.; Nurrul, A.S.; Shukur, M.F. Preparation and characterization of solid biopolymer electrolytes based on polyvinyl alcohol/cellulose acetate blend doped with potassium carbonate (K₂CO₃) salt, *J. Electroanal. Chem.* **2022**, *919*, 116539, <https://doi.org/10.1016/j.jelechem.2022.116539>.

8. Khan, N.M.; Mazuki, N.M.; Abdul Majeed, A.P.P.; Samsudin, A.S. Interrelation Between Ionic Conduction and Ions Fraction of Biopolymer Electrolytes Based on Alginate Doped with NH₄Cl, *J. of Macromol. Sci, Part B*, **2021**, *60*, 631-646, <https://doi.org/10.1080/00222348.2021.1889126>.
9. Maheshwari, T.; Tamilarasan, K.; Selvasekarapandian, S.; Chitra, R.; Muthukrishnan, M. Synthesis and characterization of Dextran, poly (vinyl alcohol) blend biopolymer electrolytes with NH₄NO₃, for electrochemical applications, *Int. J. Green Energy*, **2022**, *19*, 314-330, <https://doi.org/10.1080/15435075.2021.1946811>.
10. Sengwa, R. J.; Priyanka, D.; Shobhna, C. Effects of plasticizer and nanofiller on the dielectric dispersion and relaxation behaviour of polymer blend based solid polymer electrolytes. *Current Applied Physics*. 2015, *15*, 135-143, <https://doi.org/10.1016/j.cap.2014.12.003>.
11. Ryusuke, T.; Reto, M.; Laurence, J.; Frank, S.; Cordula, S.; Susanne. Formulating Amorphous Solid Dispersions: Impact of Inorganic Salts on Drug Release from Tablets Containing Itraconazole-HPMC Extrudate. *Mol Pharm*. **2020**, *17*, 2768-2778, <https://doi.org/10.1021/acs.molpharmaceut.9b01109>.
12. Kumar, S.; Dongre, S.; Raghu, S.; Demappa, T.; Sannappa, J. Structural and Mechanical characteristic study of HPMC polymer composite films, Second International Conference on Physics of Materials and Nanotechnology, Mangalore University, India, 27/10/2021 - 30/10/2021, *IOP Conf. Ser.: Mater. Sci. Eng.* **2022**, *1221*, 012011, <https://doi.org/10.1088/1757-899X/1221/1/012011>.
13. Kumar, S.; Demappa, T.; Sannappa, J. Influence of KI salt concentration on the hydroxypropyl methylcellulose films: Optical study, *Opt. Mater.* **2022**, *129*, 112474, <https://doi.org/10.1016/j.optmat.2022.112474>.
14. Cyriac, V.; Ismayil, Noor, I.M.; Mishra, K.; Chavan, C.; Bhajantri, R.F.; Masti, S.P. Ionic conductivity enhancement of PVA: carboxymethyl cellulose poly-blend electrolyte films through the doping of NaI salt. *Cellulose*, **2022**, *29*, 3271–3291, <https://doi.org/10.1007/s10570-022-04483-z>.
15. Abdullah, A.M.; Aziz, S.B.; Saeed, S.R. Structural and electrical properties of polyvinyl alcohol (PVA): Methyl cellulose (MC) based solid polymer blend electrolytes inserted with sodium iodide (NaI) salt, *Arab. J. Chem.* **2021**, *14*, 103388, <https://doi.org/10.1016/j.arabjc.2021.103388>.
16. Shetty, S.K.; Ismayil; Hegde, S.; Ravindrachary, V.; Sanjeev, G.; Bhajantri R.F.; Masti, S.P. Dielectric relaxations and ion transport study of NaCMC:NaNO₃ solid polymer electrolyte films. *Ionics*, **2021**, *27*, 2509–2525, <https://doi.org/10.1007/s11581-021-04023-y>.
17. Bharati, D.C.; Rawat, P.; Saroj, A.L. Structural, thermal, and ion dynamics studies of PVA-CS-NaI-based biopolymer electrolyte films. *J Solid State Electrochem*, **2021**, *25*, 1727-1741, <https://link.springer.com/article/10.1007/s10008-021-04946-6>.
18. Shetty, S.K.; Ismayil, N.; Swathi, M.M.G.; Rashmitha, K. Sodium ion conducting PVA/NaCMC bio poly-blend electrolyte films for energy storage device applications. *Int. J. Polym. Anal. Charact.* **2021**, *26*, 411–424, <https://doi.org/10.1080/1023666X.2021.1899685>.
19. Michael, J.D.; Henry J.B.; Theodore J.B.; David C.S. "Bromine Compounds" in Ullmann's Encyclopedia of Industrial Chemistry Wiley-VCH, Weinheim, **2000**, <https://onlinelibrary.wiley.com/doi/book/10.1002/14356007>.
20. Fuentes, I.; Andrio, A.; Teixidor, F.; Viñas, C.; Compañ, V. Enhanced conductivity of sodium versus lithium salts measured by impedance spectroscopy. Sodium cobaltacarboranes as electrolytes of choice. *Phys. Chem. Chem. Phys.* **2017**, *19*, 15177–15186, <https://doi.org/10.1039/C7CP02526B>.
21. Rani, N.S.; Sannappa, J.; Demappa, T.; Mahadevaiah. Structural, thermal, and electrical studies of sodium iodide (NaI)-doped hydroxypropyl methylcellulose (HPMC) polymer electrolyte films. *Ionics*. **2014**, *20*, 201–207, <https://doi.org/10.1007/s11581-013-0952-8>.
22. Ravi, M.; Pavani, Y.; Kiran, K. K.; Bhavani, S.; Sharma, A. K.; Narasimha Rao, V.V.R. Studies on electrical and dielectric properties of PVP:KBrO₄ complexed polymer electrolyte films. *Materials Chemistry and Physics*, 2011, *130*, 442-448, <https://doi.org/10.1016/j.matchemphys.2011.07.006>.
23. Kumar, S.; Raghu, S.; Demappa, T.; Sannappa, J. Effect of NaBr on the Structural, Thermal and Mechanical Properties of HPMC:NaBr Composite Films. *Asian J. Chem.* **2022**, *34*, 305-310, <https://doi.org/10.14233/ajchem.2022.23507>.
24. Andrew, K. J. Relaxation in low-loss dielectrics. *Journal of Molecular Liquids*, 2000, *86*, 259-268. [https://doi.org/10.1016/S0167-7322\(99\)00147-6](https://doi.org/10.1016/S0167-7322(99)00147-6).
25. Jonscher, A. K. Dielectric Relaxation in low loss Solids. *J molec liqu.* **2000**, *86*, 259–268, [https://doi.org/10.1016/S0167-7322\(99\)00147-6](https://doi.org/10.1016/S0167-7322(99)00147-6).

26. Rani, M. S. A.; Mohamed, N. S.; Isa, M. I. N. (2015) Investigation of the Ionic Conduction Mechanism in Carboxymethyl Cellulose/Chitosan Biopolymer Blend Electrolyte Impregnated with Ammonium Nitrate. *International Journal of Polymer Analysis and Characterization*, 2015, 6, 491-503, <https://doi.org/10.1080/1023666X.2015.1050803>,
27. Kiran, K.K.; Ravi, M.; Pavani, Y.; Bhavani, S.; Sharma, A.K.; Rao, V.V.R.N. Investigations on the effect of complexation of NaF salt with polymer blend (PEO/PVP) electrolytes on ionic conductivity and optical energy band gaps, *Physica B*, **2011**, 406, 1706-1712, <https://doi.org/10.1016/j.physb.2011.02.010>.
28. Kim, C.; Lee, G.; Lio, K.; Ryu, K.S.; Kang, S.G.; Chang, S.H. Polymer electrolytes prepared by polymerizing mixtures of polymerizable PEO-oligomers, copolymer of PVDC and poly(acrylonitrile), and lithium triflate, *Solid State Ion*, **1999**, 123, 251-257, [https://doi.org/10.1016/S0167-2738\(99\)00119-8](https://doi.org/10.1016/S0167-2738(99)00119-8).
29. Lee, K. H.; Kim, H. Y.; La, Y. M.; Lee, D. R. Sung, N. H. Influence of a mixing solvent with tetrahydrofuran and N, N-dimethylformamide on electrospun poly(vinyl chloride) nonwoven mats. *J Polym Sci and Polym Phys*, **2002**, 40, 2259–2268, <https://doi.org/10.1002/polb.10293>.
30. Han, Y.G.; Kusunose, T.; Sekino, T. One-step reverse micelle polymerization of organic dispersible polyaniline nanoparticles. *J Synth Mater* **2009**, 159, 123–131, <https://doi.org/10.1016/j.synthmet.2008.08.011>.
31. Aziz, S.B.; Abdullah O.Gh.; Saeed S.R.; Hameed M.A. Electrical and dielectric properties of copper ion conducting solid polymer electrolytes based on chitosan: CBH model for ion transport mechanism, *Int. J. Electrochem. Sci.* **2018**, 13, 3812 – 3826, <https://doi.org/10.20964/2018.04.10>.
32. Sahoo, S.; Hajra, S.; Mohantha, K.; Choudhary, R. N. P. Processing dielectric and impedance spectroscopy of lead free BaTiO₃, BiFeO₃ CaSnO₃, *J. Alloy. Comp.* **2018**, 766, 25–32, <http://dx.doi.org/10.1016/j.jallcom.2018.06.284>.
33. Ibrahim, S.; Yasin, S.M.M.; Nee, N.M.; Ahmad, R.; Johan, M.R. Conductivity and dielectric behavior of PEO-based solid nanocomposite polymer electrolyte, *J. Soli. Sta. Commun*, **2012**, 152, 426-434, <https://doi.org/10.1016/j.ssc.2011.11.037>.
34. Jonscher, A.K. The Universal dielectric response, *J. Nature*, **1977**, 267, 673-679, <https://doi.org/10.1038/267673a0>.
35. Ramesh, S.; Liew, C.W. Exploration on nano-composite fumed silica-based composite polymer electrolytes with doping of ionic liquid, *J. Non-Cryst. Soli.* **2012**, 358, 931-940, <https://doi.org/10.1016/j.jnoncrysol.2012.01.005>.
36. Funke, K. Jump relaxation in solid electrolytes, *J. Prog. Solid State Chem*, **1993**, 22, 111-195, [https://doi.org/10.1016/0079-6786\(93\)90002-9](https://doi.org/10.1016/0079-6786(93)90002-9).
37. Maji; Pande, P.P.; Choudary, R.B. Effect of Zn(NO₃)₂ filler on the dielectric permittivity and electrical modulus of PMMA, *J. Bull. Mater. Sci.* **2015**, 38, 417-424, <https://doi.org/10.1007/s12034-015-0886-z>.
38. Ranjan, R.; Kumar, R.; Kumar, N.; Behera, B.; Choudhary, R. N. P. Impedance and electric modulus analysis of Sm-modified Pb(Zr_{0.55}Ti_{0.45})_{1-x/4}O₃ ceramics, *J. Alloy. Compd*, **2011**, 509, 6388-6394, <https://doi.org/10.1016/j.jallcom.2011.03.003>.
39. Aziz, S. B.; Rasheed, M. A.; Abidin, Z. H. Z. Optical and electrical characteristics of silver ion conducting nanocomposites solid polymer electrolytes based on chitosan, *J. Electron. Mater.* **2017**, 46, 6119-6130, <https://doi.org/10.1007/s11664-017-5515-8>.